Nuclear Structure Studies in the Palladium Isotopes with (d,p) and (d,t) Reactions*

BIBIJANA ČUJEC
University of Pittsburgh, Pittsburgh, Pennsylvania
(Received 18 March 1963)

Many new energy levels are located in the odd-A palladium isotopes and the spin and parity values assigned. The parameters of the pairing theory, such as the single quasiparticle energies, the occupation numbers, the strength of the pairing interaction, etc., are evaluated. By means of them, the single-particle energies are obtained and compared with other nuclei of the same neutron shell. While the orbits $2d_{5/2}$, $3s_{1/2}$, and $2d_{3/2}$ do not change their relative locations significantly, the $1g_{7/2}$ orbit shows drastic changes. In the palladium isotopes the $1g_{7/2}$ orbit is found to be below the $2d_{5/2}$ orbit, while in zirconium it is as high as the $2d_{3/2}$ orbit, and in tin somewhat above the $2d_{5/2}$ orbit. This indicates that the interaction between the $1g_{7/2}$ neutrons and the $1g_{9/2}$ protons, which causes the shift of the $1g_{7/2}$ orbit, is most effective in palladium isotopes, i.e., where the $1g_{9/2}$ proton orbit is about half-full. The strength of the pairing interaction is evaluated to be $GA=29.2\pm0.9$ MeV.

INTRODUCTION

IT has been shown by Cohen[1] and Talmi[2] that the single-particle energies do not always show a regular dependence on the mass number. The drastic shifts observed for some orbits have been explained as due to the interaction between protons and neutrons, which is especially strong between neutrons and protons of the same l. While the strong, short-range interaction between identical nucleons within the same orbit is very successfully accounted for by the pairing theory, there is no theory yet for the strong and short-range interaction between neutrons and protons. As one effect of this interaction is just the shifts of the single-particle energies, it is of high interest to locate the single-particle energies in as many nuclei as possible, not only at the beginnings and ends of the closed shells, but also far from closed shells.

It has been shown by Sorensen[3] and by Yoshida[4] that the pairing theory is well applicable also in vibrational nuclei, like palladium, although in these nuclei many levels of the same single-particle j value appear because of the coupling of this single-particle state with the phonon state of the even-even core. Thus, the present work contributes, in addition to the previous work on zirconium,[5] tin,[6] barium and cerium,[7] to our understanding of the nuclei with neutrons in the 50–82 shell, consisting of $2d_{5/2}$, $2d_{3/2}$, $3s_{1/2}$, $1g_{7/2}$, and $1h_{11/2}$ orbits.

EXPERIMENT AND RESULTS

The isotopes Pd^{104}, Pd^{106}, and Pd^{108} were bombarded with 15-MeV deuterons from the Pittsburgh cyclotron. The targets were about 3 mg/cm² thick and about 90% pure in the isotope being investigated. The reaction products were analyzed by the magnetic spectrometer and detected with photographic plates. Some typical spectra of protons and tritons are shown by Figs. 1 and 2. The resolution is ~30 keV for protons and ~50 keV for tritons; the center of each peak is, however, located with an accuracy of ~8 keV.

As a subsidiary result, the ground-state reaction Q values (Table I) have been obtained. The absolute $Q(d,p)$ values are accurate within 0.1 MeV, while the differences are accurate within 0.02 MeV, since they have been obtained from the relative positions of the ground-state peaks in the proton spectrum of a natural palladium target. For $Q(d,t)$ both absolute values and differences are accurate within 0.1 MeV. The uncertainties in the best previous data[8] are about 0.4 MeV.

The proton spectra were recorded at angles of 10°, 20°, and 33°. Calculations of the angular distributions, performed in distorted-wave Born (DWB) approximation (Fig. 3), show that it is very easy to distinguish between the transferred angular momentum values $l=0$, $l=2$, and $l=4$ or $l=5$, by possessing just the cross-section values at 10°, 20°, and 33°. It is, however, not possible to distinguish between $l=4$ and $l=5$ values. Moreover, the cross sections are in these both cases rather low and the corresponding peaks are expected to be often screened by the $l=0$ and $l=2$ peaks.

TABLE I. Q values for (d,p) and (d,t) reactions in Pd isotopes.

Target	$Q(d,p)$-MeV This work	$Q(d,p)$-MeV Previous[a]	$Q(d,t)$-MeV This work	$Q(d,t)$-MeV Previous[a]
104	4.580	4.56	−3.53	−3.58
105	7.350	7.35		−0.53
106	4.291	4.14	−3.32	−3.32
108	3.903	3.87	−2.97	−2.91

[a] Ref. 8.

* Supported by the Office of Naval Research and the National Science Foundation.

[1] B. L. Cohen, Phys. Rev. **127**, 597 (1962).
[2] I. Talmi, Rev. Mod. Phys. **34**, 704 (1962).
[3] R. A. Sorensen, Nucl. Phys. **25**, 674 (1961).
[4] S. Yoshida, Nucl. Phys. **38**, 380 (1962).
[5] B. L. Cohen, Phys. Rev. **125**, 1358 (1962).
[6] B. L. Cohen and R. E. Price, Phys. Rev. **121**, 1441 (1961).
[7] R. H. Fulmer, A. L. McCarthy, and B. L. Cohen, Phys. Rev. **128**, 1302 (1962).
[8] V. J. Ashby and M. C. Catron, *Tables of Nuclear Reaction Q Values*, University of California Radiation Laboratory Report 5419, 1959 (unpublished).

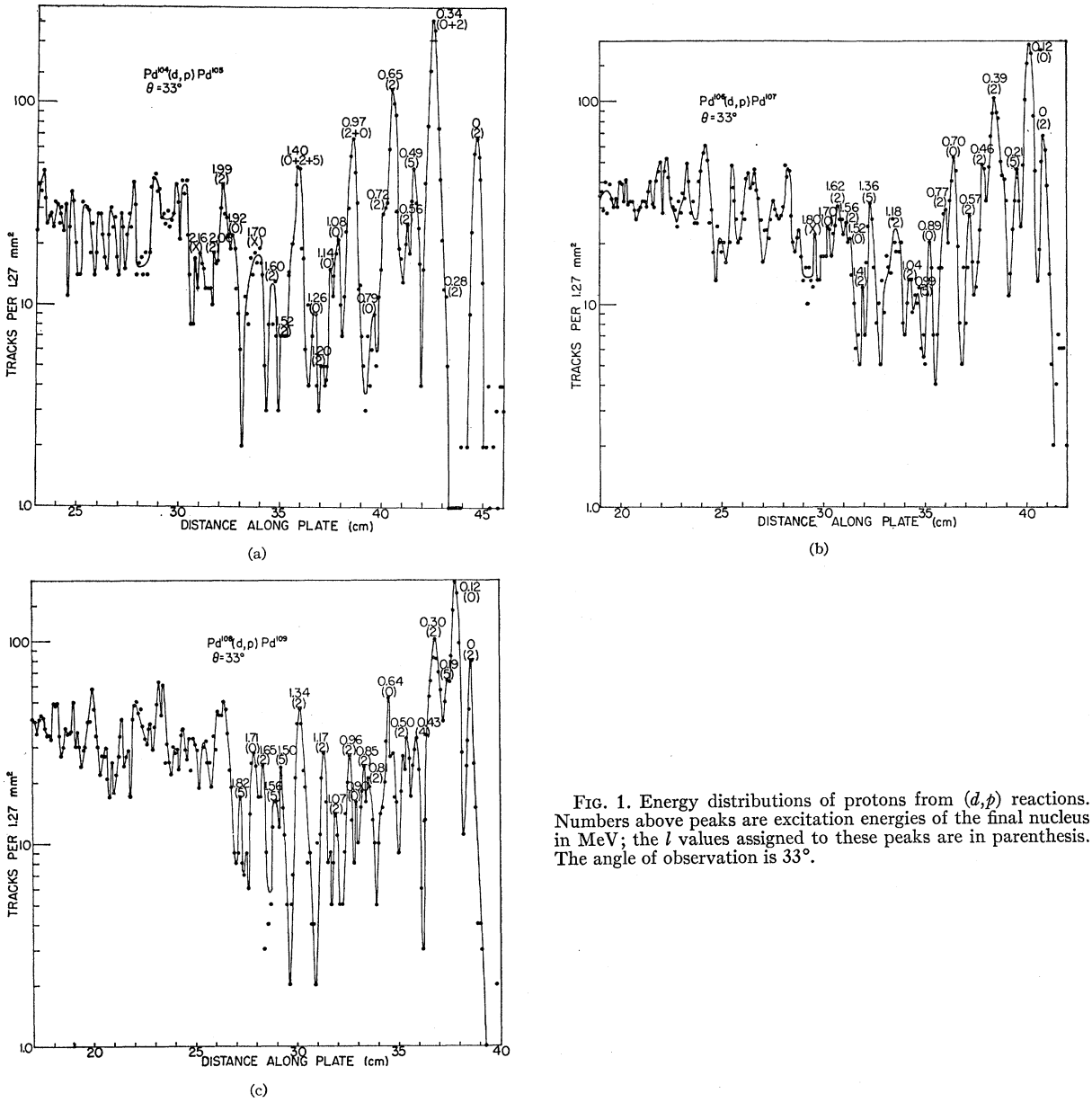

FIG. 1. Energy distributions of protons from (d,p) reactions. Numbers above peaks are excitation energies of the final nucleus in MeV; the l values assigned to these peaks are in parenthesis. The angle of observation is 33°.

To decide whether an $l=2$ neutron has been put into the $2d_{5/2}$ or the $2d_{3/2}$ orbit the cross sections for (d,p) and (d,t) reactions, leading to the same final state, have been compared. Since the $2d_{5/2}$ orbit is lower and therefore more full than the $2d_{3/2}$ orbit, the ratio between (d,p) and (d,t) cross sections is much smaller for a $2d_{5/2}$ neutron than for a $2d_{3/2}$ neutron. The distinction between $2d_{5/2}$ and $2d_{3/2}$ orbits is quite clear whenever both (d,p) and (d,t) cross sections have been measured, as is the case with Pd^{105} and Pd^{107}. In the case of Pd^{109}, where the only available data are from the $Pd^{108}(d,p)Pd^{109}$ reaction, the orbits $2d_{5/2}$ and $2d_{3/2}$ have been assigned according to the cross-section sums, and by analogy with Pd^{105} and Pd^{107} levels.

With the l_j value of the transferred neutron, the spin and the parity of the final state, are also determined. Since the target nuclei have $J=0^+$, the spin of the final state is equal to the j value of the transferred neutron. Whether the l value is odd or even determines the parity. Thus, quite complete information about nuclear levels in the odd-A Pd isotopes has been obtained up to about 2-MeV excitation energy. The results are presented in Table II and in Fig. 4.

For Pd^{103} the only available data are from $Pd^{104}(d,t)Pd^{103}$ reaction. No DWB calculations have been carried out for tritons, yet the angular distributions are known from previous[6] measurements on tin isotopes. Although the angular distributions are

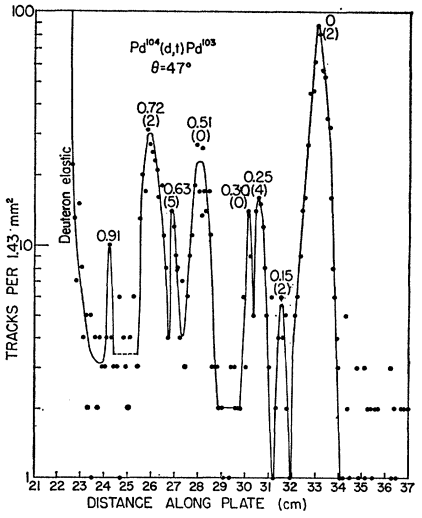

(a)

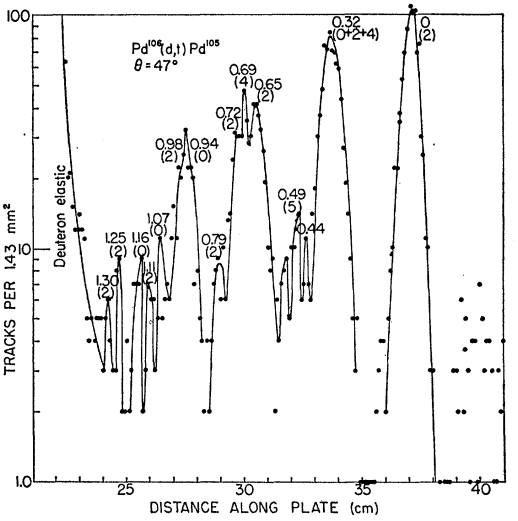

(b)

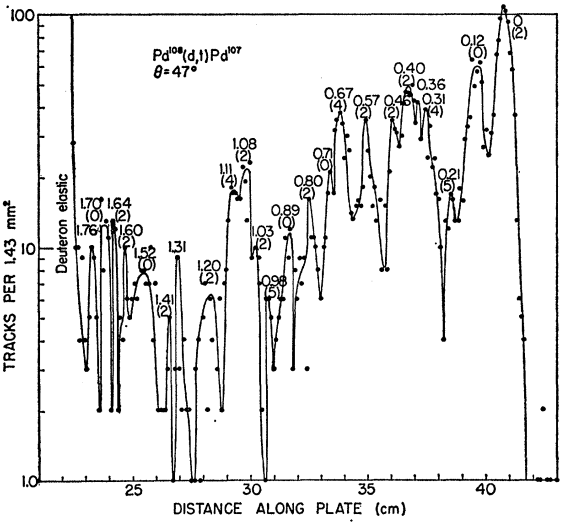

(c)

FIG. 2. Energy distributions of tritons from (d,t) reactions. Numbers above peaks are excitation energies of the final nucleus in MeV; the l values assigned are in parentheses. The angle of observation is 47°.

not as distinct as in the case of protons, the l values of picked-up neutrons can be rather safely determined by comparing the cross sections measured at 22°, 35°, 47°, and 59° with given[6] angular distributions, and comparing cross-section values with those of the other Pd isotopes. The ground state of Pd^{103} is found to be a $d_{5/2}$ state. This contradicts the ground-state spin value $\frac{7}{2}^+$, which has been proposed[9] from the ft value for β decay. The possibility that the ground-state peak includes both a $d_{5/2}$ level and a $g_{7/2}$ level is not excluded by the present experiment, although it does not seem probable. On the other hand, the evidence for $\frac{7}{2}^+$ spin value is quite inconclusive. It has previously only been inferred from the Pd^{103} ground-state β decay to the Rh^{103} level with $J=\frac{7}{2}^+$. The log ft value is 5.8, suggesting

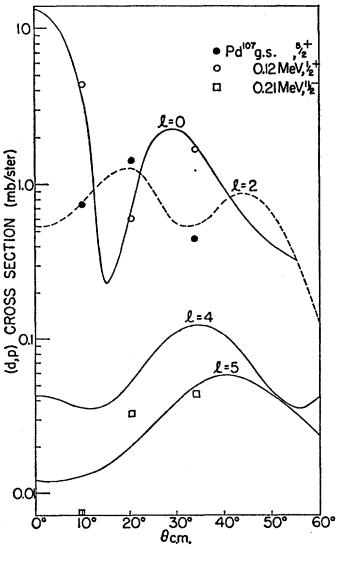

FIG. 3. Angular distributions for protons from (d,p) reactions with different angular momentum transfer (l). The curves represent the single-particle cross sections obtained by DWB calculations, and the points show experimental measurements. The scale (mb/sr) refers to the single-particle cross sections in the case of $Q=4$ MeV.

[9] *Nuclear Data Sheets*, compiled by K. Way *et al.* (Printing and Publishing Office, National Academy of Sciences–National Research Council, Washington 25, D. C., 1960).

TABLE II. Energy levels with spin values for Pd isotopes, obtained from (d,p) and (d,t) reactions leading to the given isotope as final nucleus, together with (d,p) and (d,t) cross sections leading to the given energy level.

NDS[a]	Energy level (MeV) (d,p)	Energy level (MeV) (d,t)	l[c]	J^π	$d\sigma/d\Omega$ (mb/sr)[b] (d,p)	$d\sigma/d\Omega$ (mb/sr)[b] (d,t)
		Pd^{103}				
g.s. $(7/2^+)$		g.s.	2	$5/2^+$		0.80
(0.15)		0.151	2	$(5/2)^+$		0.04
(0.26)		0.252	4	$7/2^+$		0.13
		0.297	0	$1/2^+$		0.07
		0.510	0	$1/2^+$		0.32
		0.627	5	$11/2^-$		0.09
		0.721	2	$3/2^+$		0.39
		0.907				0.04
		Pd^{105}				
g.s. $5/2^+$	g.s.	g.s.	2	$5/2^+$	1.60	1.11
0.280 $(3/2^+)$	0.280	···	2	$3/2^+$	0.08	···
0.306 $(7/2^+)$			4	$7/2^+$	···	0.20
0.319 $(7/2^+,5/2^+)$		0.321	2	$5/2^+$	0.34	0.24
0.344 $(1/2^+)$	0.340		0	$1/2^+$	3.24	0.53
0.444	···	0.441				0.04
0.489 $(11/2^-)$	0.486	0.486	5	$11/2^-$	0.37	0.10
0.561	0.565	···	2	$3/2^+$	0.30	···
0.651 (3/2,1/2)	0.651	0.652	2	$3/2^+$	2.27	0.33
	···	0.692	4	$7/2^+$	···	0.19
0.723	0.724	0.721	2	$5/2^+$	0.17	0.15
0.785	0.787	0.785	0	$1/2^+$	0.08	0.05
		0.939	0	$1/2^+$	0.25	0.13
	0.970	0.979	2	$3/2^+$	1.02	0.14
	1.075	1.068	0	$1/2^+$	0.16	0.04
	1.103	1.105	2	$3/2^+$	0.17	0.03
	1.141	1.155	0	$1/2^+$	0.07	0.04
	1.201	1.242	2	$3/2^+$	0.06	0.03
	1.263	1.288	0	$1/2^+$	0.09	0.02
			2	$3/2^+$	0.37	
	1.402	1.417	0	$1/2^+$	0.44	0.04
			5	$11/2^-$	0.11	
	1.522		2	$3/2^+$	0.15	
	1.602		2	$3/2^+$	0.19	
	1.652		x[c]		0.14	
	1.702		x[c]		0.15	
	1.772		x[c]		0.31	
	1.867		2	$3/2^+$	0.13	
	1.923		0	$1/2^+$	0.27	
	1.990		2	$3/2^+$	0.61	
	2.062		2	$3/2^+$	0.15	
	2.102		x[c]		0.14	
	2.613		x[c]		0.18	
		Pd^{107}				
g.s. $(5/2)^+$	g.s.	g.s.	2	$5/2^+$	1.59	0.99
	0.115	0.115	0	$1/2^+$	3.34	0.53
0.216 $(11/2^-)$	0.209	0.208	5	$11/2^-$	0.44	0.09
0.306	0.306	0.311	4	$7/2^+$	0.10	0.20
		0.362				0.23
0.390	0.386	0.401	2	$3/2^+$	2.50	0.23
	0.463	0.458	2	$3/2^+$	0.90	0.12
	0.574	0.570	2	$5/2^+$	0.54	0.25
0.65	···	0.665	(4)	$(7/2^+)$		0.27
	0.703	0.706	0	$1/2^+$	0.74	0.09
	0.770		2	$3/2^+$	0.36	
	0.815	0.796	···	···		0.10
	0.889	0.891	0	$1/2^+$	0.19	0.06
	0.991	(0.981)	5	$11/2^-$	0.14	0.02
	1.039	1.029	2	$3/2^+$	0.17	0.05
	1.086	1.078	2	$5/2^+$	0.10	0.10
	···	1.104	(4)	$(7/2^+)$	···	0.09
	1.184	1.200	2	$3/2^+$	0.74	0.08
	1.358	···	5	$11/2^-$	0.36	···
	···	1.303	x[c]	x[c]	···	0.03
	1.411	1.402	2	$3/2^+$	0.13	0.01
	1.471	···	2	$3/2^+$	0.13	···
	1.521	1.510	0	$1/2^+$	0.26	0.08
	1.563	1.589	2	$3/2^+$	0.22	0.03
	1.621	1.632	2	$3/2^+$	0.42	0.03
	1.701	1.689	0	$1/2^+$	0.19	0.05
	1.754	1.753	x[c]	x[c]	0.14	0.03
	1.798		x[c]	x[c]	0.17	
		Pd^{109}				
g.s. $5/2^+$	g.s.		2	$5/2^+$	1.34	
	0.115		0	$1/2^+$	2.70	
0.18	0.188		5	$11/2^-$	0.23	
	0.297		2	$3/2^+$	2.21	
	0.431		(4)	$(7/2^+)$	0.17	
	0.497		2	$(5/2)^+$	0.47	
	0.527		4, 5	$(11/2^-)$	0.15	
	0.615		4, 5	$(11/2^-)$	0.18	
	0.642		0	$1/2^+$	0.61	
	0.807		2	$(3/2)^+$	0.34	
	0.848		2	$(3/2)^+$	0.37	
	0.901		0	$1/2^+$	0.10	
	0.961		2	$(3/2)^+$	0.39	
	1.065		2	$(3/2)^+$	0.15	
	1.126		0	$1/2^+$	0.09	
	1.166		2	$(3/2)^+$	0.28	
	1.226		0	$1/2^+$	0.09	
	1.338		2	$3/2^+$	0.81	
	1.498		4, 5	$(11/2^-)$	0.16	
	1.556		4, 5	$(11/2^-)$	0.13	
	1.651		2	$(3/2)^+$	0.19	
	1 710		0	$1/2^+$	0.29	
	1.777		x[c]	x[c]	0.10	
	1.823		4, 5	$(11/2^-)$	0.10	

[a] Ref. 9.
[b] For (d,p) reactions, the listed cross sections are averages over 10°, 20°, and 33° for l values 0 and 2, and they are averages over 20° and 33° degrees for l values 4 and 5. For (d,t) reactions, the given cross sections are at 47°.
[c] Notation x means: Identification of l value was not possible. In all these cases the cross section is decreasing with angle of observation.

l-allowed transition ($\Delta l=0$). Nevertheless, the transition Rh^{105}, $\frac{7}{2}^+ \xrightarrow{\beta^-}$ Pd^{105}, $\frac{5}{2}^+$, which is an l-forbidden transition ($\Delta l=2$), also has a log ft value equal to 5.7. The angular distributions for levels at 0.252 and 0.625 MeV suggest $l=4$ or $l=5$. The first level is assigned to be $1g_{7/2}$, and the second level to be $1h_{11/2}$, according to their cross-section values, which are expected to be larger for $1g_{7/2}$ neutrons than for $1h_{11/2}$ neutrons.

As is seen from Fig. 4, one level—usually the lowest one—is more strongly excited in both (d,p) and (d,t) reactions than any other with the same j. This level we shall call the simple single quasiparticle level. The energies of these simple single quasiparticle levels are represented in Fig. 5. It is remarkable that the $3s_{1/2}$, $2d_{3/2}$, and $1h_{11/2}$ levels are decreasing with increasing number of neutrons, while the $1g_{7/2}$ level is increasing.

The sums of cross sections involving transitions to all levels with the same l_j are presented in Table III,

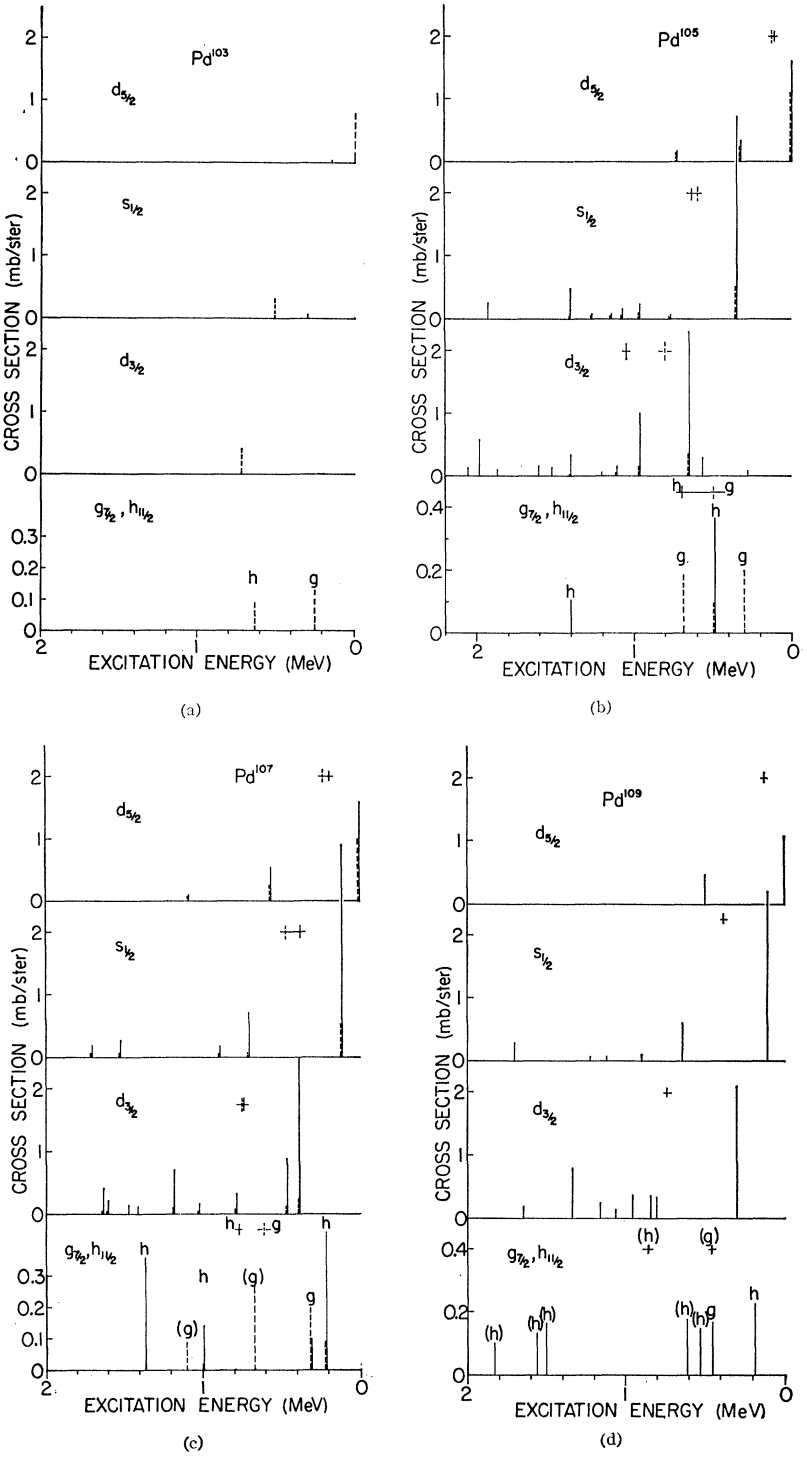

FIG. 4. Energy levels with (d,p) and (d,t) cross sections. The (d,p) cross sections represent averages over 10°, 20°, and 33°, and are shown by a solid line. The (d,t) cross sections are at 47° and are shown by a dashed line. Note the different scale for $1g_{7/2}$ and $1h_{11/2}$ cross sections. The solid and dashed crosses show the (d,p) and (d,t) barycenters, respectively.

together with cross sections involving transitions to the simple single quasiparticle level. It is seen that the other levels contribute appreciably in all cases except $Pd^{104}(d,t)Pd^{103}$. Here essentially only the simple single quasiparticle levels are excited. This indicates that Pd^{103} may be regarded as composed of a neutron and a rather inert core of Pd^{102}. For $_{46}Pd_{56}^{102}$, which has six neutrons in the 50–82 shell, the most inert configuration for neutrons is $(2d_{5/2})^6$. This configuration has been established very clearly[5] for $_{40}Zr_{56}^{96}$. As we shall see later, the present measurements show that the $1g_{7/2}$ orbit is located below the $2d_{5/2}$ orbit in all directly

TABLE III. Cross sections (mb/sr) for (d,p) and (d,t) reactions leading to the simple single quasiparticle level, and to all levels of the same single-particle orbit.

	$d\sigma_j{}^0(d,p)/d\Omega$			$\Sigma_n d\sigma_j{}^n(d,p)/d\Omega$			$d\sigma_j{}^0(d,t)/d\Omega$			$\Sigma_n d\sigma_j{}^n(d,t)/d\Omega$		
Target mass	104	106	108	104	106	108	104	106	108	104	106	108
$2d_{5/2}$	1.60	1.59	1.34	2.11	2.23	1.81	0.80	1.11	0.95	0.84	1.50	1.35
$3s_{1/2}$	3.24	3.34	2.70	4.60	4.72	3.88	0.32	0.53	0.53	0.39	0.84	0.81
$2d_{3/2}$	2.27	2.50	2.21	5.55	5.57	4.74	0.39	0.33	0.23	0.39	0.53	0.65
$1g_{7/2}$	···	0.10	0.17	···	>0.10	0.17	0.13	0.20	0.20	0.13	0.39	(0.56)
$1h_{11/2}$	0.37	0.44	0.23	0.48	0.94	0.95	0.09	0.10	0.09	0.09	0.10	0.11

measured palladium isotopes, Pd^{104}, Pd^{106}, and Pd^{108}. One possible explanation is that at the beginning of the shell the $2d_{5/2}$ orbit is the lowest one and well separated from the other orbits. When the shell, however, contains about 8 or more neutrons, the $1g_{7/2}$ orbit approaches to the $2d_{5/2}$ orbit, and in Pd isotopes it comes even below the $2d_{5/2}$ orbit.

INTERPRETATION OF EXPERIMENTAL RESULTS IN TERMS OF THE PAIRING THEORY

1. Pairing Theory

The pairing theory developed by Belyaev[10] and Kisslinger and Sorensen[11] takes into account the strong, attractive, short-range two-body interaction which acts between identical nucleons coupled to spin 0. By virtue of this interaction all even-even nuclei have in their ground states $J=0$, and in addition many of them have an energy gap of ~ 2 MeV between the ground state and the first excited state. The pairing interaction causes strong configuration mixing among the low-lying shell-model wave functions. Consequently, the nucleons do not occupy only the lowest possible single particle energy orbits as they would in the absence of any residual interaction, but all orbits of the shell, which is filling, are partially occupied. The occupation number V_j^2 gives the probability that orbit j is occupied, and the complementary U_j^2 gives the probability that orbit j is empty. Thus, the number of neutrons (we want to consider neutron shells) in the j orbit is

$$n_j=(2j+1)V_j^2, \tag{1}$$

and

$$V_j^2+U_j^2=1. \tag{2}$$

The ground state of an even-even nucleus is represented by the so-called vacuum, which is analogous to a closed shell. Instead of unperturbed single-particle energies, ϵ_j, the single quasiparticle energies, E_j, are introduced, and in such a way that the energy of an excited state is equal to the sum of all single quasiparticle energies. They are related to unperturbed single-particle energies by

$$E_j=[(\epsilon_j-\lambda)^2+\Delta^2]^{1/2}, \tag{3}$$

where λ is the surface of the Fermi sea, or the so-called chemical potential, and Δ is approximately the energy of the lowest single quasiparticle level, measured from the vacuum. (See Fig. 6.)

Actually, the pairing theory introduces just one new parameter, the strength of the pairing interaction, G. All other parameter are expressible in terms of ϵ_j, G, and the number of neutrons in the unfilled shell, n. Thus, parameters λ and Δ are obtainable from the two fundamental equations:

$$\frac{G}{2}\sum_j \frac{2j+1}{[(\epsilon_j-\lambda)^2+\Delta^2]^{1/2}}=1, \tag{4}$$

$$\tfrac{1}{2}(2j+1)\left[1-\frac{\epsilon_j-\lambda}{[(\epsilon_j-\lambda)^2+\Delta^2]^{1/2}}\right]=n, \tag{5}$$

where the summation refers to the vacuum.

The occupation numbers V_j^2 and U_j^2 of the vacuum state are given by

$$V_j^2=\frac{1}{2}\left[1-\frac{\epsilon_j-\lambda}{[(\epsilon_j-\lambda)^2+\Delta^2]^{1/2}}\right]$$
$$U_j^2=\frac{1}{2}\left[1+\frac{\epsilon_j-\lambda}{[(\epsilon_j-\lambda)^2+\Delta^2]^{1/2}}\right]. \tag{6}$$

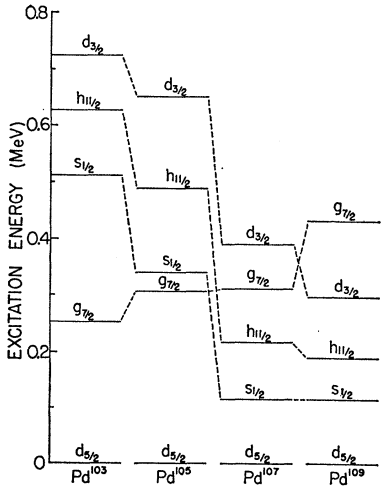

FIG. 5. Simple single quasiparticle energy levels in Pd isotopes.

[10] S. T. Belyaev, Kgl. Danske Videnskab. Selskab, Mat. Fys. Medd. **31**, No. 11 (1959).
[11] L. S. Kisslinger and R. A. Sorensen, Kgl. Danske Videnskab. Selskab, Mat. Fys. Medd. **32**, No. 9 (1960).

From (3) and (6) we get a relation between E_j and V_j^2:

$$E_j=\frac{\Delta}{2V_jU_j}=\frac{\Delta}{2[V_j^2(1-V_j^2)]^{1/2}}. \quad (7)$$

Considering relation (3) we get for the lowest single quasiparticle energy, which is the energy of the ground state of the next odd-even nucleus,

$$E_g\approx(E_j)_{\min}=\Delta, \quad (8)$$

and from (7) there than follows the occupation number

$$V_g^2\approx\tfrac{1}{2}. \quad (9)$$

Thus, the same orbit, which gives the ground state of the odd-even nucleus, is about half-full in the preceding even-even nucleus. The occupation of orbits decreases with increasing ϵ_j or in other words, a higher orbit is always less occupied than a lower one. Adding neutrons into a shell, the single-particle energies ϵ_j move down with respect to the surface of the Fermi sea. The consequence is that the single quasiparticle energies E_j corresponding to orbits below the Fermi surface move up, and that E_j corresponding to orbits above the Fermi surface move down (see Fig. 6). Thus, Fig. 5 shows that in the Pd isotopes, the $1g_{7/2}$ orbit lies below the Fermi surface, while all the other orbits (except $2d_{5/2}$ in some isotopes) lie above the Fermi surface.

Actually, the only known parameter is n, the number of neutrons outside the closed shells, while the single-particle energies, ϵ_j, and the strength of the pairing force G, have to be determined by experiment.

2. Parameters of the Pairing Theory Obtained from (d,p) and (d,t) Reactions

The (d,p) and (d,t) reactions are excellent tools to study the neutron single-particle levels, because in the first approximation the interaction involved is just the interaction between the transferred neutron and the nuclear potential well. In the case where the target is a closed shell nucleus the replacement of the nucleus by a potential well is especially justified. In this case, the (d,p) reactions lead just to the single-particle levels and the (d,t) reactions to the single-hole levels of that potential well.

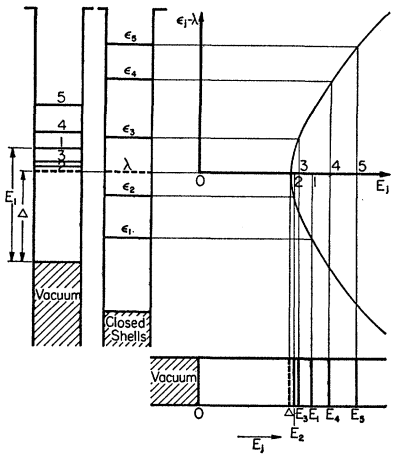

FIG. 6. Scheme illustrating relation between the single-particle energy levels ϵ_j and the single quasiparticle energy levels E_j: $E_j=[(\epsilon_j-\lambda)^2+\Delta^2]^{1/2}$.

TABLE IV. Single-particle cross sections (mb/sr).

Orbit	$\epsilon_j-\epsilon_{5/2}$ (MeV)	$[d\sigma_l(d,p)/d\Omega]_{s.p.}$[a]			$[d\sigma_l(d,t)/d\Omega]_{s.p.}$[b]		
$2d_{5/2}$	0	0.66	0.70	0.73	0.35	0.39	0.47
$3s_{1/2}$	1.37	1.89	1.91	1.98	3.68	3.22	3.81
$2d_{3/2}$	2.67	1.21	1.29	1.41	1.03	1.15	1.36
$1g_{7/2}$	0	0.07	0.08	0.09	0.09	0.10	0.12
$1h_{11/2}$	3.46	0.07	0.07	0.08	0.18	0.20	0.24
Target mass		104	106	108	104	106	108

[a] The values are averages over 10°, 20°, and 33° for l values 0 and 2, and they are averages over 20° and 33° for l values 4 and 5. They have been calculated by DWB approximation with the single-particle energy levels as given in the second column.
[b] The values refer to 47° and have been obtained experimentally.

In the pairing theory, all even-even nuclei play the roles of closed shell nuclei, and the single-quasiparticle energies take the roles of the single-particle energies. Thus, in the absence of any other residual interaction but pairing, with (d,p) and (d,t) reactions on even-even target nuclei just the single-quasiparticle states will be excited. However, there also exists among all the nucleons a long-range interaction (often approximated by a quadrupole force). This interaction gives rise to vibrational (phonon) states in the even-even nuclei and, by coupling phonons with particles, splits a given single-particle level into more levels. This is evident within the Pd isotopes (see Fig. 4), which are, as is well known, in a vibrational region. The simple single-quasiparticle level involves no phonons, but the other, weakly excited levels arise from one- and two-phonon interactions with the single-quasiparticle state. Fortunately, there exist sum rules,[4] which enable us to determine the unperturbed single-quasiparticle energies, E_j, and occupation numbers, V_j^2 in terms of the observed energy levels, E_j^n and spectroscopic factors, S_j^n.

The spectroscopic factor S gives the overlap between the initial and final wave functions and depends only on the nuclear states involved. We shall consider only the cases, where the initial state is the ground state of an even-even nucleus with $J=0$, and we shall specify the final state by the reaction symbol (d,p) or (d,t), by the single-particle state j, and by an additional parameter n. The observed cross sections are related to spectroscopic factors as

$$d\sigma_j^n(d,p)/d\Omega=[d\sigma_l(d,p)/d\Omega]_{s.p.}(2j+1)S_j^n(d,p), \quad (10a)$$

and

$$d\sigma_j^n(d,t)/d\Omega=[d\sigma_l(d,t)/d\Omega]_{s.p.}S_j^n(d,t), \quad (10b)$$

where the first factor on the right-hand side represents the single-particle cross section, which can be calculated in different approximations. For (d,p) reactions it has been obtained by DWB calculations. Results are presented in Table IV together with the single-particle

binding energies, to which the calculated cross sections refer. For (d,t) reactions, the single-particle cross sections have been obtained experimentally by comparing the measured (d,p) and (d,t) cross sections involving transitions between the same two nuclear states. Thus, the (d,t) single-particle cross section for $l=2$ was obtained from $Pd^{105}(d,p)Pd^{106}$ g.s. and $Pd^{106}(d,t)Pd^{105}$ g.s. transitions, and for $l=0$ it was obtained from $Cd^{113}(d,p)Cd^{114}$ g.s. and $Cd^{114}(d,t)Cd^{113}$ g.s. transitions. The (d,t) single-particle cross sections for $l=4$ and $l=5$ were obtained by assuming that the cross section is proportional to 2^{-l}.

According to Yoshida[4]

$$\sum_n (2j+1)S_j^n(d,p)=(2j+1)U_j^2 + (2\lambda+1)\sum_{j'}(\phi_{jj',a}^{\lambda})^2 V_j^2 \quad (11a)$$

and

$$\sum_n S_j^n(d,t)=(2j+1)V_j^2 + (2\lambda+1)\sum_{j'}(\phi_{jj',a}^{\lambda})^2 U_j^2, \quad (11b)$$

where $\phi_{jj',a}^{\lambda}$ is the amplitude of the two-quasiparticle term contributing to the phonon state of order λ and energy $\hbar\omega_a$. All quantities on the right-hand side refer to the even-even (target) nucleus. The vibrational term [containing $\sum_{j'}(\phi_{jj',a}^{\lambda})^2$] is presumably small and may be neglected except in the case of very small V_j^2 or U_j^2. Equations (11) without the vibrational term are identical with sum rules given by Macfarlane and French.[12]

By adding both Eqs. (11) together and considering (2) we get

$$\sum_n (2j+1)S_j^n(d,p)+\sum_n S_j^n(d,t) = 2j+1+(2\lambda+1)\sum_{j'}(\phi_{jj',a}^{\lambda})^2, \quad (12)$$

a relation, from which the vibrational term can be obtained, in principle. Computing the left-hand side of the equation by dividing the sums of the cross sections (Table III) by the single-particle cross sections (Table IV) we get a value which is only 5 to 20% different from $2j+1$. These computed values are usually larger than $2j+1$ and have been estimated for $2d_{5/2}$, $2d_{3/2}$, and $3s_{1/2}$ orbits. The uncertainty of the result is, however, larger than 20% because the error in the experimental cross section is about 10%, and in the calculated single-particle cross sections probably at least 20%.

Neglecting the vibrational term in (11), the occupation numbers V_j^2 have been determined for all orbits, except $1g_{7/2}$, from the experimental values for $\sum_n d\sigma_j^n(d,p)/d\Omega$ and $\sum_n d\sigma_j^n(d,t)/d\Omega$, and from single-particle cross sections as given by Table IV. The occupation number $V_{7/2}^2$ cannot be obtained by the same procedure, since most of the $1g_{7/2}$ levels are not observed. It has been determined by the condition

$$\sum_j (2j+1)V_j^2=n,$$

where n is the number of neutrons in the filling shell. The numerical results are presented in Table V. To check the pairing theory, occupation numbers obtained from quasiparticle energies E_j according to relation (7) are also listed. The agreement with directly obtained V_j^2 values is fairly good. The results, obtained by either of the two methods, show that the $1g_{7/2}$ orbit is more occupied than the $2d_{5/2}$ orbit. This is additional evidence that the $1g_{7/2}$ orbit is below the $2d_{5/2}$ orbit.

The relations between the single-quasiparticle energies E_j and the observed energies E_j^n are[4]

$$\sum_n E_j^n(2j+1)S_j^n(d,p)=(2j+1)\Big[E_jU_j^2 - 2\Big(\frac{2\lambda+1}{2j+1}\Big)^{1/2}\sum_{j'}\langle j|H|j'\lambda,j\rangle\phi_{jj',a}^{\lambda}U_jV_j + \frac{2\lambda+1}{2j+1}\sum_{j'}(E_{j'}+\hbar\omega_a)(\phi_{jj',a}^{\lambda})^2V_j^2\Big] \quad (13a)$$

and

$$\sum_n E_{j'}{}^nS_j^n(d,t)=(2j+1)\Big[E_{j'}V_j^2 + 2\Big(\frac{2\lambda+1}{2j+1}\Big)^{1/2}\sum_{j'}\langle j|H|j'\lambda,j\rangle\phi_{jj',a}^{\lambda}U_jV_j + \frac{2\lambda+1}{2j+1}\sum_{j'}(E_{j'}+\hbar\omega_a)(\phi_{jj',a}^{\lambda})^2U_j^2\Big], \quad (13b)$$

TABLE V. Number of neutrons in individual orbits, n_j, and occupation numbers V_j^2.

	$n_j=(2j+1)V_j^2$			V_j^2			$V_j^2(E_j)$[a]		
Target mass	104	106	108	104	106	108	104	106	108
$2d_{5/2}$	2.54	3.17	3.30	0.424	0.529	0.550	~0.5	~0.5	~0.5
$3s_{1/2}$	0.12	0.19	0.19	0.060	0.095	0.095	0.12	0.16	0.18
$2d_{3/2}$	0.31	0.40	0.44	0.077	0.100	0.110	0.09	0.12	0.13
$1g_{7/2}$	4.67[b]	5.65[b]	7.19[b]	0.584[b]	0.705[b]	0.899[b]	>0.78[c]	>0.79[c]	>0.81[c]
$1h_{11/2}$	~0.35	~0.59	~0.88	0.030	0.050	0.080	<0.13	<0.12	0.12
$\Sigma_j n_j$	8.00	10.00	12.00						

[a] V_j^2 determined from E_j values as obtained by Yoshida's method (Table VI) and with parameter $\Delta^j=1.53$ MeV.
[b] Determined by the condition that the sum $\Sigma_j n_j$ is equal to the total number of neutrons in the shell.
[c] Lower limit, determined from $E_{7/2}{}^0$.

[12] M. H. Macfarlane and J. B. French, Rev. Mod. Phys. **32**, 567 (1960).

TABLE VI. Single-quasiparticle energy levels, E_j(MeV), measured from the ground state of the odd-even (final) nucleus, as obtained by different methods.

Method	Yoshida[a]			(d,p) barycenter			(d,t) barycenter			E_j^0			
Final isotope				105	107	109	103	105	107	103	105	107	109
Target isotope	104	106	108	104	106	180	104	106	108				
$2d_{5/2}$	0.06	0.17	0.16	0.11	0.19	0.13	0.01	0.12	0.23	0	0	0	0
$s_{1/2}$	0.81	0.55	0.43	0.63	0.38	0.39	0.47	0.60	0.48	0.511	0.340	0.115	0.115
$d_{3/2}$	1.27	0.89	0.71	1.05	0.74	0.74	0.72	0.80	0.75	0.724	0.651	0.390	0.297
$g_{7/2}$	···	···	···	···	(0.31)	0.43	0.25	0.50	0.61	0.252	0.306	0.311	0.431
$1h_{11/2}$	>0.44	>0.85	0.92	0.70	0.77	0.86	0.63	···	0.36	0.629	0.489	0.216	0.188

[a] Determined according to Eq. (15).

where all energies are measured from the vacuum state. The last term on the right-hand side is negligible, while the middle term is not necessarily small. Applying both Eqs. (13) to the same target nucleus and assuming equality of the single-quasiparticle energies in the two final nuclei ($E_j=E_j'$), although these differ in number of neutrons by two, we obtain by adding the equations

$$\sum_n E_j^n(2j+1)S_j^n(d,p)+\sum_n E_{j'}^n S_{j'}^n(d,t) \approx (2j+1)E_j+(2\lambda+1)\sum_{j'}(E_{j'}+\hbar\omega_a)(\phi_{jj',a}^{\lambda})^2. \quad (14)$$

Neglecting the last term and inserting spectroscopic factors from (10) we have

$$(2j+1)E_j\approx\sum_n \frac{E_j^n d\sigma_j^n(d,p)/d\Omega}{[d\sigma_l(d,p)/d\Omega]_{\text{s.p.}}} +\sum_n \frac{E_{j'}^n d\sigma_{j'}^n(d,t)/d\Omega}{[d\sigma_l(d,t)/d\Omega]_{\text{s.p.}}}. \quad (15)$$

We see that so calculated E_j values depend on experimental and single-particle cross sections for both (d,p) and (d,t) reactions. In the previous work,[5-7] the E_j values have been obtained as barycenters of levels, excited in either (d,p) or (d,t) reactions. They are defined as

$$E_j(d,p)=\frac{\sum_n E_j^n S_j^n(d,p)}{\sum_n S_j^n(d,p)}\approx\frac{\sum_n E_j^n d\sigma_j^n(d,p)/d\Omega}{\sum_n d\sigma_j^n(d,p)/d\Omega}, \quad (16)$$

and

$$E_j(d,t)=\frac{\sum_n E_j^n S_j^n(d,t)}{\sum_n S_j^n(d,t)}\approx\frac{\sum_n E_j^n d\sigma_j^n(d,t)/d\Omega}{\sum_n d\sigma_j^n(d,t)/d\Omega}. \quad (17)$$

The relation (16) follows from relations (13a) and (11a), and the relation (17) follows from relations (13b) and (11b), if both the quadratic and linear vibrational terms in (13) and (11) are neglected.

While from the theoretical point of view, Eq. (15) represents a better approximation for E_j than Eq. (16) or (17), the last two methods express E_j in terms of directly measured quantities only. Therefore, the single-quasiparticle energies have been determined by all three methods, and the numerical results are shown in Table VI. For comparison also the simple single quasiparticle energies E_j^0 are included.

In principle, it is possible to calculate the term $\sum_{j'}\langle j|H|j'\lambda,j\rangle\phi_{jj',a}^{\lambda}$. From Eqs. (13) and (16) we get

$$\sum_{j'}\langle j|H|j'\lambda,j\rangle\phi_{jj',a}^{\lambda} =[E_j-E_j(d,p)]\frac{(2j+1)^{3/2}}{2(2\lambda+1)^{1/2}}\frac{U_j}{V_j}. \quad (18)$$

The numerical results for $2d_{3/2}$ and $3s_{1/2}$ orbits are shown in Table VII. They do not show a regular variation with the number of neutrons and therefore do not seem reliable. Probably, the single-particle cross sections are not enough accurate, but also the $E_j(d,p)$ and $E_j(d,t)$ do not vary in a regular manner with the number of neutrons.

Possessing the values for V_j^2 and E_j the determination of the remaining parameters of the pairing theory is straightforward.

The single-particle energies, ϵ_j, with respect to the $\epsilon_{5/2}$ are determined from Eq. (3) or better from the diagram shown in Fig. 6. (Notice that to each value for E_j there are two possibilities for ϵ_j.) For E_j, the numerical values obtained by (15) have been used.

The parameter Δ, or more correctly the energy of the single-quasiparticle ground state, E_g, measured from the vacuum, is obtained from differences in separation energies, S.E., between the adjacent even and odd isotopes:

$$2\Delta(n)\approx 2E_g(n)=\tfrac{1}{2}\{|\text{S.E.}(n)-\text{S.E.}(n-1)| +|\text{S.E.}(n)-\text{S.E.}(n+1)|\}. \quad (19)$$

The values for separation energies have been taken from the *Tables of Nuclear Reaction Q Values*.[8]

The location of the Fermi surface with respect to the ground-state single-particle energy, ϵ_g, is obtained from Eqs. (6) and (3).

$$\epsilon_g-\lambda=E_g(1-2V_g^2). \quad (20)$$

TABLE VII. Values for $\sum_{j'}\langle j|H|j'\lambda,j\rangle\phi_{jj',a}^{\lambda}$.

Isotope	104	106	108
$3s_{1/2}$	0.44	0.33	0.08
$2d_{3/2}$	1.36	0.81	−0.15

TABLE VIII. Parameters of the pairing theory for Zr, Pd, and Sn isotopes.

Reference	Isotope	Zr[91,92] [a]	Zr[94] [a]	Zr[96,97] [a]	Pd[104] [b]	Pd[106] [b]	Pd[108] [b]	Sn[116] [c]	Sn[118] [c]	Sn[120] [c]	Sn[122] [c]	Sn[124] [c]
	$2d_{5/2}$	0.30	0.62	0.96	0.42	0.53	0.55	0.79	0.80	0.87	0.86	0.93
	$3s_{1/2}$	0.05	0.05	0.05	0.06	0.10	0.10	0.42	0.52	0.61	0.69	0.74
V_j^2	$2d_{3/2}$	···	0.05	0.05	0.08	0.10	0.11	0.25	0.33	0.55	0.59	0.68
	$1g_{7/2}$	<0.03	<0.04	<0.06	0.58	0.71	0.90	0.78	0.86	0.89	(0.92)	(0.95)
	$1h_{11/2}$	···	···	···	0.03	0.05	0.08	0.27	0.33	0.35	0.47	0.55
	$2d_{5/2}$	0	0	···	0	0	0	0	0	0	0	0
	$3s_{1/2}$	1.55	2.1	0	1.48	1.17	1.09	1.65	1.72	1.57	1.40	1.37
ϵ_j(MeV) [d]	$2d_{3/2}$	2.70	3.3	1.37	2.06	1.65	1.59	2.45	2.12	1.87	1.85	1.94
	$1g_{7/2}$	2.70	3.3	1.64	<−1.2	<−0.5	<−0.8	0.42	0.37	0.22		
	$1h_{11/2}$	>5.1	···	>4.0	>1.2	>1.6	1.85	2.75	2.32	2.12	2.05	1.94
$E_{g.s.}\sim\Delta$	(MeV)	0.86	0.85	0.92	1.28	1.50	1.47	1.13	1.36	1.37	1.32	1.34
$\epsilon_{g.s.}-\lambda$	(MeV)	0.35	−0.19	−1.04	0.23	−0.09	−0.15	0.18	0.00	−0.14	−0.24	−0.13
λ [d]	(MeV)	−0.35	0.19	1.04	−0.23	0.09	0.15	1.47	1.72	2.01	2.09	2.07
GA/Δ					19.9	19.3	20.6	16.8	17.2	18.1	18.4	20.6
GA	(MeV)				28.8	28.2	30.8	19.0	23.4	24.8	24.3	27.6

[a] Ref. 5; B. L. Cohen, Rev. Mod. Phys. (to be published).
[b] Present work.
[c] Ref. 6.
[d] Measured from $2d_{5/2}$ orbit.
[e] V_j^2 values refer to the even isotope, ϵ_j to the odd isotope.

The strength of the pairing force, G, follows from Eq. (4). Replacing E_j in the denominator by expression (7), we separate the dependence on Δ and get

$$\frac{G}{\Delta}=\frac{1}{2\sum_j(2j+1)U_jV_j}. \tag{21}$$

The numerical results for all these parameters are presented in Table VIII. The data for zirconium[5] and tin[6] isotopes are included, too. We see that within the same isotopes the occupation numbers V_j^2 monotonically increase with the number of neutrons. Within these nuclei of the same isotope the single-particle energies do not change significantly although they show a slight tendency to come closer together with increasing number of neutrons. The single-particle energies, however, change significantly from one to another isotope, as is best seen from Fig. 7. The most drastic is the shift of the $1g_{7/2}$ orbit; within the Zr isotopes this orbit is as high as the $2d_{3/2}$ orbit, while in the Pd isotopes it jumps below the $2d_{5/2}$ orbit, and then moves again upwards above the $2d_{5/2}$ orbit. This indicates that the interaction between $1g_{7/2}$ neutrons and $1g_{9/2}$ protons, which causes the shift of the $1g_{7/2}$ neutron orbit, is most effective in the Pd isotopes, i.e., where the $1g_{9/2}$ proton orbit is about half-full.

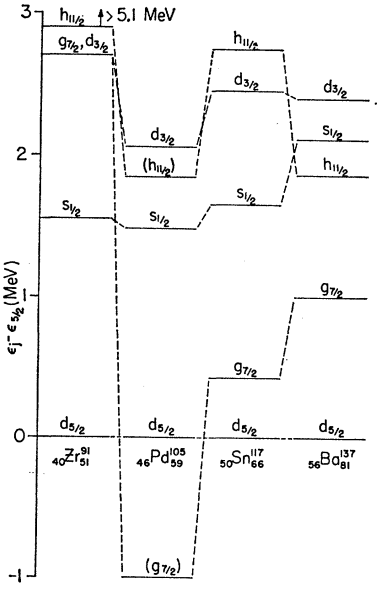

FIG. 7. Single-particle energy levels as determined by stripping and pickup reactions in nuclei within 50–82 neutron shell.

The parameter Δ is larger within Pd than within the Zr isotopes, in contrast to the general tendency of Δ, to decrease with increasing mass number. For the case of Pd^{105}, the value $\Delta=1.46\pm0.04$ MeV has been obtained from the $Q(d,p)$ values measured by the present experiment (Table I).

In the last line of Table VIII the strength of the pairing force is given in terms of GA, where A is the mass number. Within the Pd-isotopes the average value is $\langle GA\rangle_{av}=29.2\pm0.9$ MeV and within the Sn isotopes is $\langle GA\rangle_{av}=23.8\pm1.4$ MeV. These values are larger than the value ($GA=19$) assumed for Sn in Kisslinger and Sorenson[11] computations, and is in the range of the values quoted[11] for Pb isotopes ($GA=23$ to 30).

ACKNOWLEDGMENTS

The author is grateful to Frank Karasek and Ben Zeidman of Argonne National Laboratory for providing the targets on loan, and to Bernard L. Cohen, Norman Austern, and Elizabeth Baranger for many helpful discussions.